Viscous deformation of a dense well-graded gravel in different conditions

LeQuang AnhDan, University of Tokyo
Junichi Koseki, IIS, University of Tokyo
Fumio Tatsuoka, University of Tokyo

Introduction: In previous study, although gravel has been considered as a non-viscous material, AnhDan et al (2000) has shown how important creep deformation of gravel is. However, the study was performed at constant confining pressure with a partially saturated specimen. In order to have a better insight into this issue, a series of tests on a very dense well-graded gravel were performed to investigate into: the viscous property of dense gravel along different stress paths and effects of the degree on saturation on the viscous property.

Testing procedure: A large triaxial apparatus (Hoque et al., 1996) with some modifications for the purpose of the present study was used. The specimen is rectangular prismatic (58cm high and 23 cm times 23 cm in cross-section). Axial and lateral strains were measured by local displacement transducers (Goto et al., 1991) set on the surfaces of the specimen (**Fig.1**). The material used is very dense Chiba gravel with a water content of 5.5%, dry density of 2.22 to 2.23 g/cm^3 and void

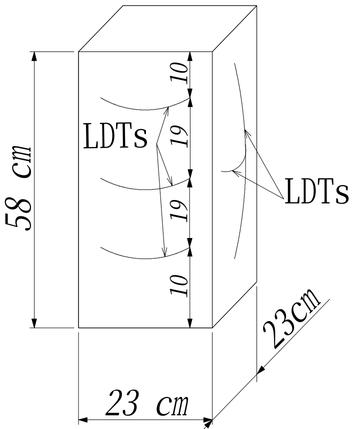

Fig.1: Large prismatic specimen

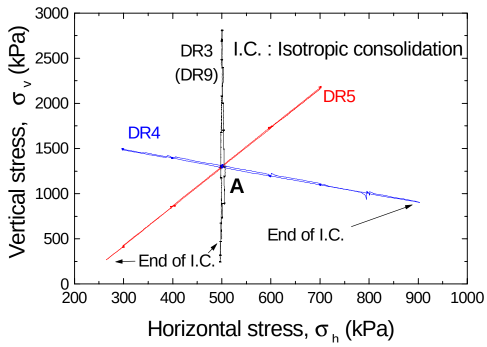

Fig. 2: Stress paths during shearing

Test name	Loading method	Saturated (S) or partially saturated (PS)	Initial dry density, void ratio	Initial degree of saturation	Stress path
DR3	Stress control	PS	2.229 g/cm^3 0.198	74.2%	***I.C.*** from 49 kPa to 490 kPa, and then ***T.C.*** at σ_h=490 kPa.
DR4	Stress control	PS	2.224 g/cm^3 0.20	73.4%	***I.C.*** from 49 kPa to 980 kPa, and then ***A.C.*** at $\Delta\sigma_v/\Delta\sigma_h$= -1.
DR5	Stress control	PS	2.226 g/cm^3 0.199	73.8%	***I.C.*** from 49 kPa to 260 kPa, and then ***A.C.*** at $\Delta\sigma_v/\Delta\sigma_h$= 4.4.
DR9	Strain control	S (B value=0.97)	2.231 g/cm^3 0.197	100 %	***I.C.*** from 49 kPa to 490 kPa, and then ***T.C.*** at σ_h=490 kPa.

Table 1
I.C.=isotropic compression; A.C.=anisotropic compression; T.C.=triaxial compression

ratio of about 0.2 before the start of consolidation. Results from three tests DR3, DR4 and DR5 using partially saturated specimens and another test DR9 using a fully saturated specimen will herein be reported. The testing conditions are shown in **Table1**. During shearing, creep deformations were allowed at different stress levels under drained conditions. Period of creep at each was about 6 hours. Stress paths of these tests are shown in **Fig. 2**.

Results and discussions: The overall relationships between the stress ratio R= σ_v/σ_h and shear strain $\gamma=\varepsilon_v-\varepsilon_h$ from tests DR3, DR4 and DR5 are shown in **Fig. 3**, while the time histories of γ are compared in **Fig. 4**. The following trends of behaviour can be seen from these figures: A considerable amount of creep strain took

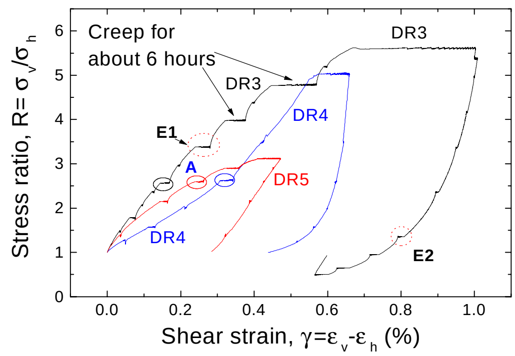

Fig. 3: Stress-strain curves during shearing

Keywords: Gravel, partially saturated , fully saturated, prismatic specimen, creep, different stress paths
IIS-University of Tokyo, Room Ce201, 4-6-1, Komaba, Meguro-ku, Tokyo, 153-8505. Tel: 03-5452-6421

place regardless of the stress paths examined. Creep strain became larger as the stress state approached the failure state and the material became more dilatant (**Fig. 6b**). When the loading was restarted at the original loading rate following each creep stage, the stress-strain curve exhibited a very stiff response, followed by marked yielding. Then, the stress-strain curve tended to rejoin the respective primary one that would have been obtained if loading had been continued without an intermission of creep loading. **Fig. 5a** shows detailed behaviour that is typical of the above. The size of high stiffness zone in the stress space developed by creep deformation increases with the increase in the creep strain. In all of three tests, at each creep stage during stress-unloading, the shear strain decreased with time (i.e., creep recovery), as typically shown in **Fig. 5b**. The amount of creep recovery became larger as the stress ratio became smaller. Immediately after unloading was restarted following each creep stage, the stress-strain curve exhibited a stiff response (Fig. 5b) in a similar manner to the one observed during loading (Fig. 5a). One may say, however, that the effect of suction is significant on such viscous property of partially saturated gravel as described above. To confirm the issue, the overall relationships between the stress ratio R= σ_v/σ_h and the shear strain γ and strain paths of the pair of partially and fully saturated specimens, from tests DR3 and DR9, are compared in **Figs. 6a & b**. It may be seen that under the present test condition at a relatively high confining pressure, the viscous deformation property of the gravel is essentially the same between the partially and fully saturated specimens.

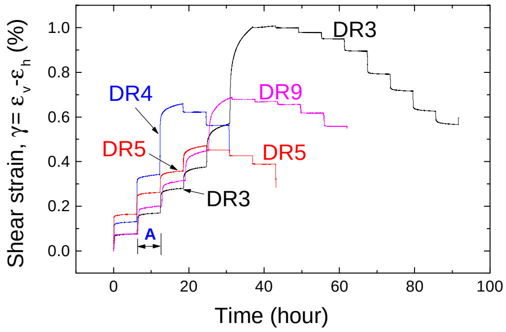

Fig. 4: Strain histories

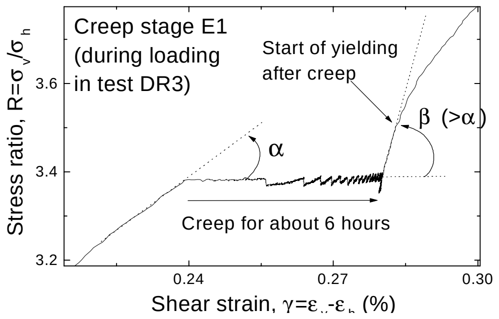

Fig. 5a: Enlargement of creep during stress-loading

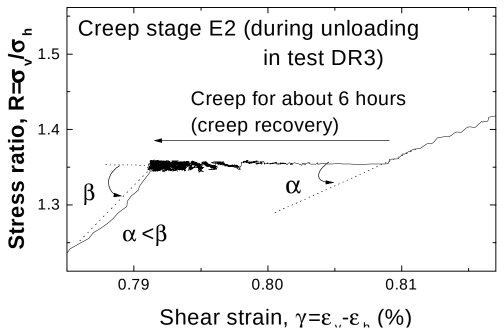

Fig. 5b: Enlargement of creep during stress-unloading

Conclusions:

At creep stages during monotonic increase and decrease of deviator stress along different stress paths on a dense well-graded gravel, significant creep deformation took place. The creep strain increased as the stress state approached the failure. The viscous deformation characteristics as well as the stress-strain behaviour were essentially the same between partially saturated and fully saturated specimens, showing insignificant effects of suction on the observed behaviour.

References: 1/AnhDan,L.Q. et al. (2000): "Creep deformation characteristics of dense gravel", 55th Annual conference of JSCE.

2/ Goto,S. et al. (1991): "A simple gauge for local strain measurements in laboratory", Soils and Foundations, Vol. 31, No. 1, pp. 169-180.

3/ Hoque,E. et al. (1996), "Measuring anisotropic elastic properties of sand using a large triaxial specimen", Geotechnical Testing Journal, ASTM, Vol.19, No.4, pp.411-420.

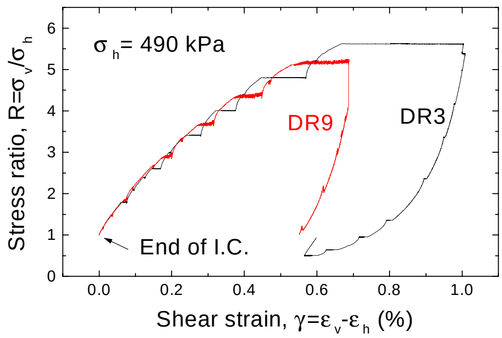

Fig. 6a: Stress-strain relationships of tests DR3 and DR9

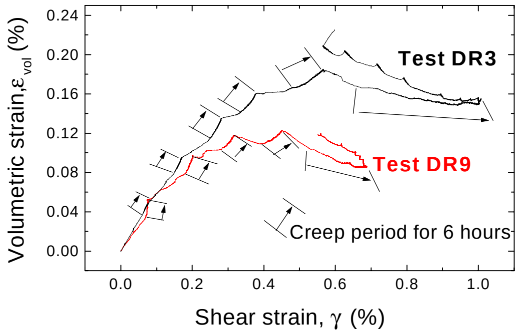

Fig. 6b: Strain paths of tests DR3 and DR9